Color Mixing Property of a Projector-Camera System

Xinli Chen* Xubo Yang† Shuangjiu Xiao‡ Meng Li§

School of Software
Shanghai Jiao Tong University, China

Abstract

In this paper, we investigate the property of how color channels of a projector-camera system interact with each other, which is also called color mixing of the system. We propose a method to describe this property with a single color mixing matrix for the system, rather than a different matrix for every surface point. The matrix is independent of projection surface and ambient light. It can be measured just like response functions of projector-camera system. The matrix is helpful for color sensitive applications like radiometric compensation and scene reconstruction. By decoupling color channels with the matrix of the system, color images can be processed on each channel separately just like gray images. As most projector-camera systems have broad overlap color channels, it's improper to neglect their interactions. We will show the validity of describing color mixing of the system with a single matrix. In the end, some experiments are designed to verify our method. The result is convincing.

CR Categories: H.5.1 [Information Interfaces and Presentation]: Multimedia Information Systems—Artificial, Augmented, and Virtual Realities; I.3.3 [Computer Graphics]: Picture/ImageGeneration—Display Algorithms

Keywords: Color Mixing, Interaction of Color Channels, System Calibration, Radiometric Compensation

1 Introduction

Projector-camera system has been used in a wide variety of applications like radiometric compensation [Nayar et al. 2003; Grossberg et al. 2004; Fujii et al. 2005; Bimber et al. 2005], tiled displays [Majumder and Stevens 2002; Majumder 2003; Raij et al. 2003], shadow elimination [Sukthankar et al. 2001; Cham et al. 2003] and so on. With its extensive usage, many works have been done to study the properties of such system. The space of camera response function was discussed and modeled by [Grossberg and Nayar 2003; Grossberg and Nayar 2004]. High-dynamic range imaging methods [Debevec and Malik 1997; Mitsunaga and Nayar 1999] are designed to measure the camera response function through a series of images captured with different but known exposures. For projector, Majumder studied its properties in the work [Majumder 2002]. The projector response function can be measured directly using a photometer [Yang et al. 2001; Majumder and Stevens 2002]. However, a photometer is prohibitively expensive as well as hard to use. Then a method adapted the high-dynamic range imaging was proposed by [Raij et al. 2003] to measure the response function using a black-white camera. These methods measured the response functions of projector and camera separately. [Song and Cham 2005] presented a theory for self-calibration of overlapping projectors and cameras. It doesn't require any expensive equipment and may be carried out with low dynamic range camera. Another method for calibration of a projector-camera system was proposed by [Juang and Majumder 2007], which measure the response functions as well as the vignetting effect.

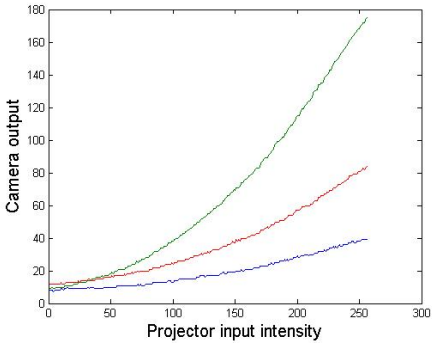

Figure 1: *Interaction of color channels. Green images with intensity from 0 to 255 (red and blue are always 0) are projected, while the red and blue channel also increase as a result of color mixing.*

The above efforts have made the using of a projector-camera system more convenient. But they deal with only gray images or treat color images simply as gray images for each channel. However, this assumption doesn't hold for most cases, as most projector-camera systems have wide overlapping color channels and the interaction is significant as shown in Figure 1. To our knowledge, color mixing of a projector-camera system is first addressed by Nayar et al. in their work [Nayar et al. 2003]. A matrix is used to capture the interactions of color channels as well as surface reflectance. As a result, the color mixing matrix varies from point to point. It's surface dependent and need to be re-evaluated for different projection surfaces. [Grossberg et al. 2004] used the color mixing matrix in a similar way. [Fujii et al. 2005] has decoupled color mixing from reflectance in their photometric model. However, they didn't measure it separately and different mixing matrices were used for different points in their proposed method.

In this paper, we propose a method to determine a single color mixing matrix for a projector-camera system, rather than a different matrix for every point. It can be regarded as a property of the projector-camera system: it is independent of projection surface or ambient light; it doesn't change dynamically unless system settings(white-balance, contrast, saturation) change. It's most useful for color sensitive applications. Take radiometric compensation for example. With the pre-determined color mixing matrix, only surface reflectance and ambient light are measured online and the compensation for color images is just as simple as for gray images.

*e-mail:chenxinl@sjtu.edu.cn
†e-mail:yangxubo@cs.sjtu.edu.cn
‡e-mail:xsjiu99@cs.sjtu.edu.cn
§e-mail:limeng@sjtu.edu.cn

PROCAMS 2008, Marina del Rey, California, August 10, 2008.
© 2008 ACM 978-1-60558-272-6/08/0008 $5.00

2 Photometric Model

As our focus is on color mixing of the system, we assume linear response functions for both projector and camera[1], each with three channels (R, G, B). We use a photometric model similar to [Nayar et al. 2003; Grossberg et al. 2004; Fujii et al. 2005] with a little modification.

There are some symbols and functions used in this model. For clarity reason, we try to keep them consistent with the original. They are listed below:

- P_K: projector brightness for channel K.
- C_L: camera captured brightness for channel L.
- λ: wavelength of visible spectrum.
- $s(\lambda)$: spectral reflectance function for a surface point in viewer's direction. We assume the reflectance is constant for each color channel. Similar assumption was also used by [Nayar et al. 2003; Song and Cham 2005; Fujii et al. 2005].
- $q_L(\lambda)$: spectral quantum efficiency function for L channel of camera.
- $e_K(\lambda, P_K)$: spectral distribution function for K channel of projector with input intensity P_K.

We start with R channel of projector for example. The irradiance on the surface point is the sum of projector illumination and ambient light. The ambient light for the point is denoted by $a(\lambda)$. Suppose the projector input intensity is P_R, then the radiance of the surface point in viewer's direction can be written as:

$$l_R(\lambda) = s(\lambda)(e_R(\lambda, P_R) + a(\lambda)). \tag{1}$$

The radiance of this point is measured with a RGB camera. The spectral quantum efficiency for the three channels are $q_R(\lambda)$, $q_G(\lambda)$, $q_B(\lambda)$ separately. As we assume reflectance for each channel is constant, denoted by (A_R, A_G, A_B), the irradiance measured by the camera for RGB channels are:

$$\begin{aligned} C_R &= A_R \int q_R(\lambda)(e_R(\lambda, P_R) + a(\lambda))d\lambda \\ C_G &= A_G \int q_G(\lambda)(e_R(\lambda, P_R) + a(\lambda))d\lambda \\ C_B &= A_B \int q_B(\lambda)(e_R(\lambda, P_R) + a(\lambda))d\lambda. \end{aligned} \tag{2}$$

We make an assumption that the spectral distribution function of projector is stable for R channel, which means:

$$e_R(\lambda, P_R) = P_R w_R(\lambda), \tag{3}$$

where $w_R(\lambda)$ is spectral response function for R channel of projector. We will verify this property in Section 3.1. With the assumption, Equation 2 can be written as:

$$\begin{aligned} C_R &= A_R \int q_R(\lambda)(P_R w_R(\lambda) + a(\lambda))d\lambda \\ C_G &= A_G \int q_G(\lambda)(P_R w_R(\lambda) + a(\lambda))d\lambda \\ C_B &= A_B \int q_B(\lambda)(P_R w_R(\lambda) + a(\lambda))d\lambda. \end{aligned} \tag{4}$$

[1] We measure the response functions for both projector and camera for each channel separately, using the method proposed by [Song and Cham 2005]. Assuming identical response function for different channels is not proper. Particularly, response functions for some projectors vary a lot for different channels.

The above process is also applicable for G and B channels of projector. At last, the photometric model of a projector-camera system at each pixel can be written as:

$$C = A(VP + F), \tag{5}$$

where

$$C = \begin{bmatrix} C_R \\ C_G \\ C_B \end{bmatrix}, A = \begin{bmatrix} A_R & 0 & 0 \\ 0 & A_G & 0 \\ 0 & 0 & A_B \end{bmatrix},$$

$$F = \begin{bmatrix} F_R \\ F_G \\ F_B \end{bmatrix}, V = \begin{bmatrix} V_{RR} & V_{GR} & V_{BR} \\ V_{RG} & V_{GG} & V_{BG} \\ V_{RB} & V_{GB} & V_{BB} \end{bmatrix}, P = \begin{bmatrix} P_R \\ P_G \\ P_B \end{bmatrix},$$

$$V_{KL} = \int q_L(\lambda) w_K(\lambda) d\lambda\,,$$

$$F_L = \int q_L(\lambda) a(\lambda) d\lambda\,.$$

The matrix A is reflectance of the surface. The vector F shows the contribution of ambient light. For convenience, the black-offset of projector is also absorbed by F. The matrix V is called color mixing matrix which describes the interaction of color channels of a projector-camera system. We will show how to determine it in next section.

3 Color Mixing of a Projector-Camera System

In this section, we first investigate the stability of spectral distribution function for projector. This property is fundamental for the model shown in Equation 5. After validation of the model, we propose a method to determine a single color mixing matrix for the system. With the determined matrix, reflectance map of a surface can be recovered with two images.

3.1 Stability of Spectral Distribution Function

We describe the method to verify stability of green channel at first; the verifications for red and blue are similar. Two uniform images are projected with different colors as:

$$P^{(0)} = \begin{bmatrix} 0 \\ 0 \\ 0 \end{bmatrix}, P^{(1)} = \begin{bmatrix} 0 \\ T \\ 0 \end{bmatrix}.$$

Applying Equation 2, we have

$$\begin{aligned} \Delta C_R &= C_R^{(1)} - C_R^{(0)} = A_R \int q_R(\lambda) e_G(\lambda, T) d\lambda \\ \Delta C_G &= C_G^{(1)} - C_G^{(0)} = A_G \int q_G(\lambda) e_G(\lambda, T) d\lambda \\ \Delta C_B &= C_B^{(1)} - C_B^{(0)} = A_B \int q_B(\lambda) e_G(\lambda, T) d\lambda\,. \end{aligned} \tag{6}$$

If the spectral distribution function is stable as shown in Equation 3, we can get the following ratios:

$$\begin{aligned} \frac{\Delta C_R}{\Delta C_G} &= \frac{A_R \int q_R(\lambda) w_G(\lambda) d\lambda}{A_G \int q_G(\lambda) w_G(\lambda) d\lambda} \\ \frac{\Delta C_B}{\Delta C_G} &= \frac{A_B \int q_B(\lambda) w_G(\lambda) d\lambda}{A_G \int q_G(\lambda) w_G(\lambda) d\lambda}\,. \end{aligned} \tag{7}$$

As the above equation shows, the ratios are independent of projector input intensities if the spectral distribution function for green

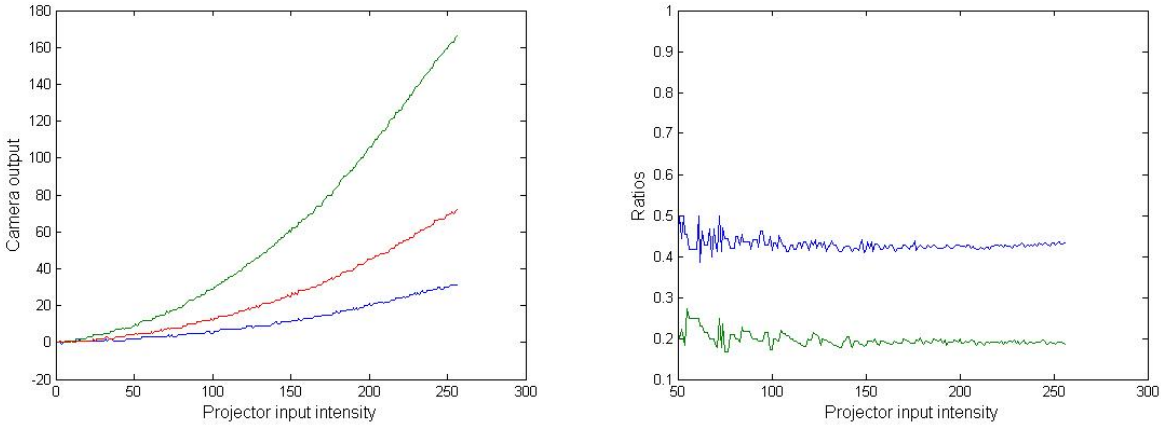

(a) (b)

Figure 2: *Stability of spectral distribution function for green channel. The left is the plot of captured data from a reference point with green channel of projector increasing from 0 to 255; the right is the plot of computed ratios, blue line for red/green and green line for blue/green*

channel of projector is stable. To verify this property, a series of 256 images with green level increasing from 0 to 255(red and blue are always 0) are projected and captured. A reference point is chosen randomly. After excluding ambient light, the captured data for this reference point is shown in Figure 2(a). We compute the ratios of this reference point for every input intensities of projector. The result is shown in Figure 2(b). It shows that the ratios do keep invariant to different projector intensities[2], which supports the assumption of stable spectral distribution function for green channel.

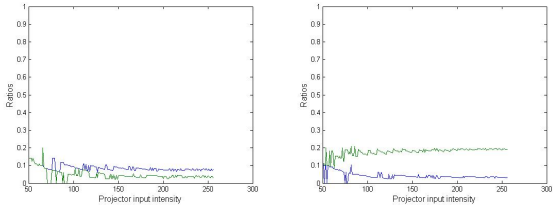

Figure 3: *The left shows the stable distribution function for red channel, and the right for blue channel.*

The verification for red and blue channels of projector is similar. The result is shown in Figure 3. With these results, we can say that the spectral distribution functions for this projector are stable for all channels. We have verified the stability for both LCD and DLP projectors, and this property is always satisfied.

3.2 Evaluation of Color Mixing Matrix

From Equation 5, as the reflectance of surface point can't be determined in advance, there's no way to measure the accurate color mixing matrix for the system. Instead, we choose a reference point, measure the combined result of AV for this point, and take the combined matrix as color mixing matrix for the system. This approxcimation is reasonable by considering the fact that the unknown scales to each row of V, caused by the reference point's reflectance A, will be absorbed by relative reflectance of other points. Suppose a reference point P_0 is chosen with combined result A_0V. For other points of the surface, we have:

$$A_iV = A_i^{'}(A_0V) \qquad i = 1, 2, \ldots \tag{8}$$

Then A_0V is used as the color mixing matrix for the system, and the surface reflectance is described by $A_i^{'}$, which is relative reflectance to the reference point.

To measure the combined result of AV, four images are projected and captured, first a black image, then a red, a green and a blue in sequence. Take red channel for example. According to Equation 5, the captured data for black image and red image is:

$$C^{(0)} = A(V\begin{bmatrix} 0 \\ 0 \\ 0 \end{bmatrix} + F) = AF,\ C^{(1)} = A(V\begin{bmatrix} P_R \\ 0 \\ 0 \end{bmatrix} + F). \tag{9}$$

Then the first column of AV can be computed as:

$$A_RV_{RR} = \frac{\Delta C_R}{P_R},\ A_GV_{RG} = \frac{\Delta C_G}{P_R},\ A_BV_{RB} = \frac{\Delta C_B}{P_R}. \tag{10}$$

Similarly, the other two columns of AV are computed with green and blue images. This method is also used by [Nayar et al. 2003; Grossberg et al. 2004; Fujii et al. 2005].

3.3 Retrieval of Reflectance Map

With the pre-determined color mixing matrix for a projector-camera system, the reflectance map of a surface can be retrieved with two images, one black $(0, 0, 0)$ and one with intensity (P_R, P_G, P_B). By excluding the ambient light from the captured gray image, we have

$$\begin{bmatrix} \Delta C_R \\ \Delta C_G \\ \Delta C_B \end{bmatrix} = \begin{bmatrix} A_R & 0 & 0 \\ 0 & A_G & 0 \\ 0 & 0 & A_B \end{bmatrix} V \begin{bmatrix} P_R \\ P_G \\ P_B \end{bmatrix}. \tag{11}$$

As V is known, we can measure the reflectance for each channel as:

$$\begin{aligned} A_R &= \frac{\Delta C_R}{V_{RR}P_R + V_{GR}P_G + V_{BR}P_B} \\ A_G &= \frac{\Delta C_G}{V_{RG}P_R + V_{GG}P_G + V_{BG}P_B} \\ A_B &= \frac{\Delta C_R}{V_{RB}P_R + V_{GB}P_G + V_{BB}P_B}. \end{aligned} \tag{12}$$

[2]The noise is mainly caused by temporally-varying projector and camera noise. The plot starts from 50 of projector input. As the camera we use has low dynamic range, captured data for low irradiance is not accurate.

4 Experiments

We use a Sony VPL-CX71 projector, a Flea2-14S3C camera. In our experiments, every scene is captured ten times and the average result is used to minimize the temporally-varying projector and camera noise.

4.1 Estimating Color Mixing Matrix

We estimate the color mixing matrix of our system on a colorful surface as shown in Figure 4. The combined result of AV is retrieved for every point of the surface using the method described in Section 3.2. We choose a white point in the center and use its combined result as the color mixing matrix for our system as shown in Figure 4.[3]

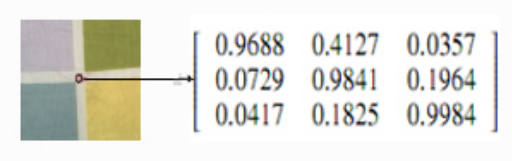

Figure 4: *Projection surface for evaluation of color mixing matrix.*

As the color mixing matrix has been determined, the relative reflectance for every point of this surface is computed according to Equation 8. There are totally 70x70 points. We expect the reflectance matrix is diagonal for every point. We take the absolute value, add them up for every element of A separately, and get a total reflectance matrix for this surface. Then the total matrix is normalized by scaling every colum with the corresponding diagonal element. The result is

$$A_{average} = \begin{bmatrix} 1.0000 & 0.0063 & 0.0012 \\ 0.0119 & 1.0000 & 0.0127 \\ 0.0046 & 0.0178 & 1.0000 \end{bmatrix}.$$

The mean error is quite small (In this case, 1.78 percent at most) as we expect. The computed reflectance map for this surface is shown in Figure 5 for RGB channels separately.

4.2 Prediction of Camera Output for a Single Point

To predict the output for a point, its reflectance is measured at first using the method proposed in Section 3.3. Then for a given projector input, the output for this point can be computed from Equation 5. We compute the camera output of this point for projector intensities from 0 to 255(gray image). For comparison, these images are also projected and captured with our projector-camera system. We choose a point from the bottom-left of the projection surface shown in Figure 4. The comparison between our prediction and real captured result is shown in Figure 6 for each channel separately. As the result shows, the prediction matches the real result very well. The average difference between prediction and real capture is 0.8518 intensity for red channel, 0.4128 intensity for green channel, and 0.4536 intensity for blue channel.

4.3 Prediction of Output Image Based on Known Input

In this section, we try to predict the camera output based on the known projector input. The prediction is done on both complex colored surface and white wall as shown in Figure 7. The reflectance

[3]Generally, a white point is chosen to be the reference point, as people tend to think white point has same reflectance for each channel. However, this is not restrictive.

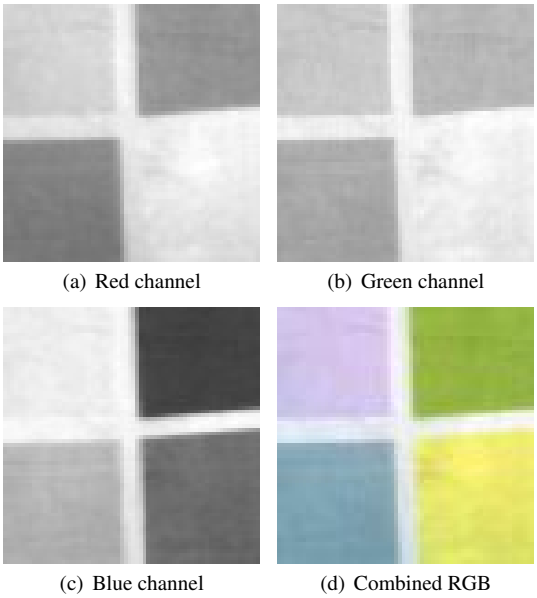

(a) Red channel (b) Green channel

(c) Blue channel (d) Combined RGB

Figure 5: *Reflectance map for the surface shown in Figure 4.*

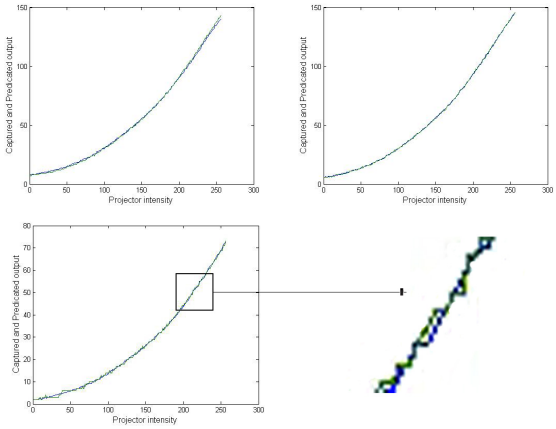

Figure 6: *Prediction of camera output for a single point for R, G, B channel with projector intensity increasing from 0 to 255.*

maps for the two surfaces are retrieved as before. The reflectance map for the colored surface is similar to the map shown in Figure 5. The reflectance map for the white wall is shown in Figure 8 for green channel; red and blue channels are similar. Note that the input to projector is a uniform gray image, and the wall is white with equal reflectance for every point. However, the relative reflectance varies from point to point, peak in the center and attenuation along the radial direction. This is because the reflectance map absorbs the vignetting effect of the projector-camera system.

With projector input intensity $(100, 200, 100)$, the real captured result and our prediction on both surfaces are shown in Figure 9. The difference maps for each channel are shown in Figure 10. The mean errors of RGB channels between prediction and real captured result are $(0.4133, 0.8466, 0.3838)$ intensities on colored surface, and $(0.3228, 0.9495, 0.5008)$ intensities on white wall. We have good reason to neglect these small errors, because of the temporally-varying projector and camera noise. We have verified the predictions for many other projector inputs. The results are quite alike, so

(a) (b)

Figure 7: *Prediction of camera output on a colored surface(a) and a white wall(b). The two images are taken with projector intensity* $(220, 220, 220)$.

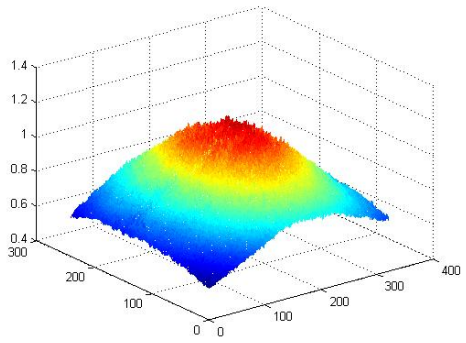

Figure 8: *Reflectance map of green channel for the white wall shown in Figure 7(b).*

we don't show them repeatedly here.

4.4 Radiometric Compensation

In this section, we illustrate the using of color mixing matrix in radiometric compensation. For radiometric compensation, the desired camera output is given; projector intensities for each point are then evaluated based on the desired output and surface reflectance. The calibration is the same as before by projecting two images. With the recovered reflectance and ambient light, projector input to produce the desired output C can be computed as:

$$P = V^{-1}(A^{-1}C - F). \tag{13}$$

First, we try to create uniform gray outputs $(80, 80, 80)$ and $(160, 160, 160)$ on a white wall. The result is shown in Figure 11. Note that the compensation image overflows in the corners for output intensity 160 because of strong vignetting effect. This problem has been addressed by [Ashdown et al. 2006; Grundhofer and Bimber 2008], and we don't cover it here. We also test on color surface. The result is shown in Figure 12.

No accurate difference maps are provided for comparison, as radiometric compensation requires accurate geometric mapping between projector points and camera points. In our experiments, we use a simple projective transformation for the mapping. Even on planar surface, noticeable displacement of pixels can be detected as a result of camera distortion.

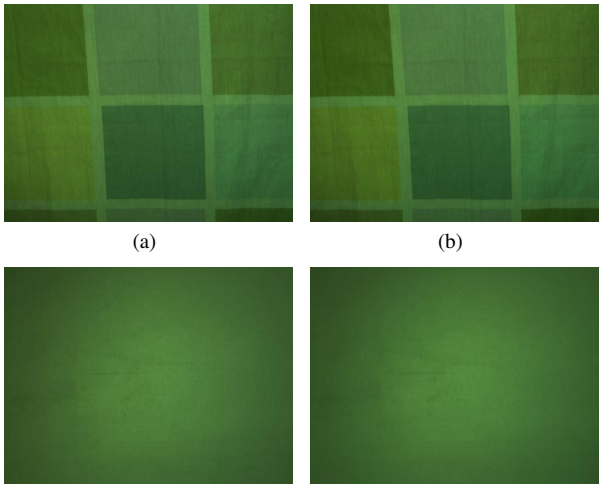

(a) (b)

(c) (d)

Figure 9: *Prediction for projector input intensity* $(100, 200, 100)$. *The left shows the real captured data, and the right shows our prediction.*

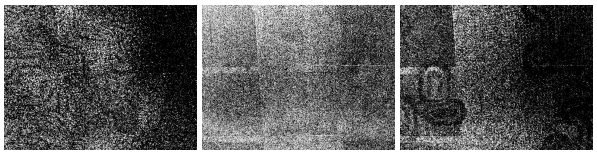

(a) Difference map of colored surface for RGB channels

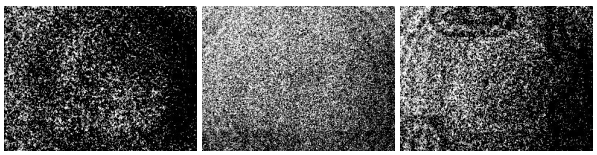

(b) Difference map of white wall for RGB channels

Figure 10: *Difference map between prediction and real captured data multiplied by 120 for both the projection surfaces with input intensity* $(100, 200, 100)$.

5 Conclusion and Future Work

We have investigated the color mixing property of a projector-camera system in this paper, and presented a method to describe this property with a single matrix. As our experiment shows, it's independent of surface reflectance, it keeps identical for every surface point, and it doesn't change dynamically unless system settings change. It simplifies the projector-camera system, and makes the using of such system more convenient, as color images can be processed just like gray images for each channel separately by decoupling with this matrix firstly.

This work has a future extension for system with multiple projectors and cameras by measuring the color mixing matrix for every pair of projector and camera. A foreseeable usage is for multi-projector display. As luminance uniform for such applications has been studied a lot, chrominance can also be considered by integrating the color mixing of the system and a better visual result can be expected.

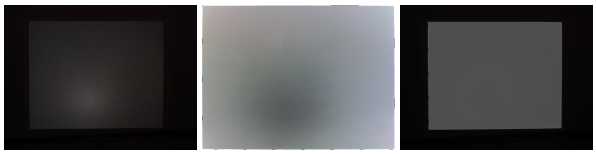

(a) Desired camera output (80, 80, 80)

(b) Desired camera output (160, 160, 160)

Figure 11: *Creating uniform gray image on white wall. left: projection without compensation; middle: compensation image; right: projection with compensation image.*

(a) projection surface

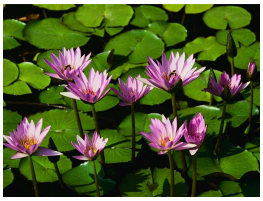

(b) original image

(c) uncompensated result

(d) compensation result

Figure 12: *Compensation of color image on color surface.*

Acknowledgements

This work was conducted at Digital Art Laboratory of Shanghai Jiao Tong University. It was sponsored by 863 National High Technology R&D Program of China (No. 2006AA01Z307).

References

ASHDOWN, M., OKABE, T., SATO, I., AND SATO, Y. 2006. Robust content-dependent photometric projector compensation. In *IEEE International Workshop on Projector-Camera Systems*, 6.

BIMBER, O., EMMERLING, A., AND KLEMMER, T. 2005. Embedded entertainment with smart projectors. *IEEE Computer 38*, 1, 48–55.

CHAM, T.-J., REHG, J. M., SUKTHANKAR, R., AND SUKTHANKAR, G. 2003. Shadow elimination and occluder light suppression for multi-projector displays. In *Proc. of CVPR*, vol. 2, 513–520.

DEBEVEC, P. E., AND MALIK, J. 1997. Recovering high dynamic range radiance maps from photographs. In *Proc. of ACM SIGGRAPH 1997*, 369–378.

FUJII, K., GROSSBERG, M. D., AND NAYAR, S. K. 2005. A projector-camera system with real-time photometric adaptation for dynamic environments. In *Proc. of CVPR*, vol. 1, 814–821.

GROSSBERG, M. D., AND NAYAR, S. K. 2003. What is the space of camera response functions? In *Proc. of CVPR*, vol. 2, 602–612.

GROSSBERG, M. D., AND NAYAR, S. K. 2004. Modeling the space of camera response functions. *IEEE Trans. Pattern Anal. Mach. Intell. 26*, 10, 1272–1282.

GROSSBERG, M. D., PERI, H., NAYAR, S. K., AND BELHUMEUR, P. N. 2004. Making one object look like another: Controlling appearance using a projector-camera system. In *Proc. of CVPR*, vol. 1, 452–459.

GRUNDHOFER, A., AND BIMBER, O. 2008. Real-time adaptive radiometric compensation. *IEEE Trans. Vis. Comput. Graph. 14*, 1, 97–108.

JUANG, R., AND MAJUMDER, A. 2007. Photometric self-calibration of a projector-camera system. In *IEEE International Workshop on Projector-Camera Systems*.

MAJUMDER, A., AND STEVENS, R. 2002. Lam: luminance attenuation map for photometric uniformity in projection based displays. In *Proc. of VRST*, ACM, 147–154.

MAJUMDER, A., JONES, D., MCCRORY, M., PAPKA, M. E., AND STEVENS, R. 2003. Using a camera to capture and correct spatial photometric variation in multi-projector displays. In *IEEE International Workshop on Projector-Camera Systems*.

MAJUMDER, A., 2002. Properties of color variation across multi-projector displays. Proc. of SID Eurodisplay.

MAJUMDER, A. 2003. *A Practical Framework to Achieve Perceptually Seamless Multi-projector Displays*. PhD thesis. The University of North Carolina at Chapel Hill.

MITSUNAGA, T., AND NAYAR, S. K. 1999. Radiometric self calibration. In *Proc. of CVPR*, 1374–1380.

NAYAR, S. K., PERI, H., GROSSBERG, M. D., AND BELHUMEUR, P. N. 2003. A projection system with radiometric compensation for screen imperfections. In *IEEE International Workshop on Projector-Camera Systems*.

RAIJ, A., GILL, G., MAJUMDER, A., TOWLES, H., AND FUCHS, H. 2003. Pixelflex2: A comprehensive, automatic, casually-aligned multi-projector display. In *IEEE International Workshop on Projector-Camera Systems*.

RASKAR, R., WELCH, G., CUTTS, M., LAKE, A., STESIN, L., AND FUCHS, H. 1998. The office of the future: A unified approach to image-based modeling and spatially immersive displays. In *Proc. of ACM SIGGRAPH 1998*, 179–188.

SONG, P., AND CHAM, T.-J. 2005. A theory for photometric self-calibration of multiple overlapping projectors and cameras. In *IEEE International Workshop on Projector-Camera Systems*, 97.

SUKTHANKAR, R., CHAM, T.-J., AND SUKTHANKAR, G. 2001. Dynamic shadow elimination for multi-projector displays. In *Proc. of CVPR*, vol. 2, 151–157.

YANG, R., GOTZ, D., HENSLEY, J., TOWLES, H., AND BROWN, M. S. 2001. Pixelflex: a reconfigurable multi-projector display system. In *Proc. of IEEE Visualization*, 167–174.